Cerebral Cortex, 2020;00: 1–15

doi: 10.1093/cercor/bhaa166
Original Article

ORIGINAL ARTICLE

The Functional Convergence and Heterogeneity of Social, Episodic, and Self-Referential Thought in the Default Mode Network

Tanya Wen[1], Daniel J Mitchell[1,†] and John Duncan[1,2,†]

[1]Cognition and Brain Sciences Unit, Medical Research Council, Cambridge CB2 7EF, UK and [2]Department of Experimental Psychology, University of Oxford, Oxford, OX2 6GG, UK

Address correspondence to Tanya Wen, Center for Cognitive Neuroscience, Duke University, LSRC, Box 90999, Durham, NC 27708, USA.
Email: tanya.wen@duke.edu
[†]Joint senior authors

Abstract

The default mode network (DMN) is engaged in a variety of cognitive settings, including social, semantic, temporal, spatial, and self-related tasks. Andrews-Hanna et al. (2010; Andrews-Hanna 2012) proposed that the DMN consists of three distinct functional–anatomical subsystems—a dorsal medial prefrontal cortex (dMPFC) subsystem that supports social cognition; a medial temporal lobe (MTL) subsystem that contributes to memory-based scene construction; and a set of midline core hubs that are especially involved in processing self-referential information. We examined activity in the DMN subsystems during six different tasks: 1) theory of mind, 2) moral dilemmas, 3) autobiographical memory, 4) spatial navigation, 5) self/other adjective judgment, and 6) a rest condition. At a broad level, we observed similar whole-brain activity maps for the six contrasts, and some response to every contrast in each of the three subsystems. In more detail, both univariate analysis and multivariate activity patterns showed partial functional separation, especially between dMPFC and MTL subsystems, though with less support for common activity across the midline core. Integrating social, spatial, self-related, and other aspects of a cognitive situation or episode, multiple components of the DMN may work closely together to provide the broad context for current mental activity.

Key words: default mode network, episodic, rest, self, social

Introduction

The default mode network (DMN) was originally discovered as a collection of medial prefrontal, lateral temporal, lateral parietal, and posterior medial cortical regions that reliably exhibit enhanced activity during passive rest compared to simple, externally oriented tasks (Shulman et al. 1997; Raichle et al. 2001). Raichle et al. (2001) postulated that the DMN is involved in cognitive states that are suspended during many attentionally demanding tasks. A large body of literature has now provided evidence that the DMN supports several aspects of spontaneous and deliberate self-generated thought that transcend the immediate sensory environment (Christoff et al. 2004, 2009; Buckner et al. 2008; Andrews-Hanna 2012; Andrews-Hanna, Smallwood, et al. 2014b). Complementing this strong activity during rest, subsequent work has shown DMN activity across a variety of high-level tasks, including social (Greene and Haidt 2002; Mars et al. 2012; Molenberghs et al. 2016), semantic (Binder et al. 2009; Humphreys and Lambon Ralph 2017), episodic (Ranganath and Ritchey 2012; Rugg and Vilberg 2013), and self-referential (Kelley et al. 2002; Chiou et al. 2019) cognition.

One common proposal is that the DMN represents broad features of a cognitive episode, scene or context (Hassabis and Maguire 2007; Ranganath and Ritchey 2012; Manning et al. 2014; Crittenden et al. 2015; Baldassano et al. 2017; Smith et al. 2018). This episode might be imagined, as in spontaneous mind-wandering or recollection of a previous event, or currently perceived (Ranganath and Ritchey 2012; Manning et al. 2014; Baldassano et al. 2017; Smith et al. 2018). Contextual representations might include spatial, social, temporal, self-related, and other features, combining to situate current cognition (Peer et al. 2015). Plausibly, there could be reduced processing of contextual features during focused attention on the details of an external task, but enhancement during spontaneous, self-generated cognition at rest.

A key question is the degree of heterogeneity across DMN regions. Early reviews (Buckner and Carroll 2007; Buckner et al. 2008), meta-analyses (Spreng et al. 2009), and experimental data (Spreng and Grady 2010) suggested that spatial, social, memory, and imagination tasks produce substantially overlapping DMN activity. More recently, consistent with the multiple features of a cognitive context, some studies suggest that the DMN exhibits heterogeneous functional components (Andrews-Hanna et al. 2010; Andrews-Hanna 2012; Andrews-Hanna et al. 2014a). In an important synthesis, Andrews-Hanna et al. (2010) partitioned the DMN into three subsystems. A dorsal medial prefrontal cortex (dMPFC) subsystem, composed of the dMPFC, the temporoparietal junction (TPJ), the lateral temporal cortex (LTC), and the temporal pole (TempP), is especially involved in "introspection about mental states", including theory of mind, moral decision making, and social reasoning. Other findings link a similar network to broader aspects of conceptual processing and semantic control (Binder et al. 2009; Andrews-Hanna et al. 2014b; Lambon Ralph et al. 2017). A medial temporal lobe (MTL) subsystem, consisting of the ventromedial prefrontal cortex (vMPFC), the posterior inferior parietal lobe (pIPL), the retrosplenial cortex, the parahippocampal cortex (PHC), and the hippocampal formation (HF+) subserves "memory-based construction/simulation", including autobiographical memory, episodic future thinking, contextual retrieval, imagery, and navigation. These two subsystems are proposed to converge on a midline core, consisting of the anterior medial prefrontal cortex (aMPFC) and the posterior cingulate cortex (PCC). The core subserves valuation of "personally significant information", as well as linking social and mnemonic processes shared with the dMPFC and MTL subsystems.

Additional studies have also emphasized that these distributed networks contain juxtaposed regions in numerous cortical zones (Peer et al. 2015; Braga and Buckner 2017), suggesting the possibility of finer scale separations within some of the DMN regions identified by Andrews-Hanna et al. (2010). For example, data from resting state connectivity (Yeo et al. 2011) suggest that only a posterior section of the pIPL might be linked to the MTL subsystem, with the more anterior section forming part of the DMN core (Andrews-Hanna et al. 2014b). Task-based analyses have shown some fractionation within single regions (Leech et al. 2011; Peer et al. 2015; Silson et al. 2019), for example, distinct PCC subdivisions may be differently sensitive to people, space, and time (Peer et al. 2015; Silson et al. 2019).

The current study further investigates separation and integration across the DMN. To this end, we examined patterns of univariate and multivoxel activity across six tasks, aiming to separate social cognition, memory-based construction/simulation, self-related cognition, and rest. Across this combination of tasks and analysis methods, we found a degree of functional separation between DMN regions, largely consistent with the Andrews-Hanna (2010) dMPFC and MTL subsystems, though less so with their concept of the midline core. However, we also found overlapping activity across the whole DMN, with each task producing some activation in each subsystem. While subsystems of the DMN system appear somewhat specialized, our data also suggest collaboration in assembling the multiple components of a cognitive situation or context.

Methods

Participants

A total of 27 participants (13 male, 14 female; ages 20–39, mean = 24.8, SD = 4.3) were included in the experiment at the MRC Cognition and Brain Sciences Unit. An additional participant was excluded due to excessive head motion (>5 mm). All participants were fluent English speakers, neurologically healthy, right-handed, with normal or corrected-to-normal vision. Participants were also required to be familiar with navigating in Cambridge city center. Procedures were carried out in accordance with ethical approval obtained from the Cambridge Psychology Research Ethics Committee, and participants provided written, informed consent before the start of the experiment.

Stimuli and Task Procedures

This study consisted of six tasks that were previously found to engage the DMN. These tasks were: a theory of mind task, a moral dilemmas task, an autobiographical memory task, a spatial imagery task, a self/other adjective judgment task, and a comparison of rest with working memory (Fig. 1). For the first five tasks, each run contained two conditions (one condition that has been associated with DMN activity and a matched control condition), along with periods of fixation between trials or blocks. Conditions were presented in randomized order, with the restriction of a maximum of two consecutive trials or blocks of the same condition. For the working memory task, each run contained alternating periods of working memory and periods of fixation. In all runs, participants were instructed to relax and clear their minds of any thought during fixation periods, and fixation periods were jittered and sampled from a random uniform distribution (see details below for each task). Before entering the scanner, participants practiced a shortened version of each task (containing one to two trials or blocks of each condition). Participants were also asked to practice writing down digital numbers until they were able to write all of them in the correct format, and to confirm that they were familiar with all 20 landmark locations used in the spatial imagery task. Inside the scanner, there were two scanning runs for each task. Run order was randomized with the constraint that repeats of the same task were between four and seven runs apart. Before the start of each run, participants were played audio-recorded task instructions to remind them of what to do during that run. Each run lasted approximately 5–7 minutes.

All tasks were coded and presented using the Psychophysics Toolbox (Brainard 1997) in Matlab 2014a (The MathWorks, Inc.). Stimuli were projected on a 1920 × 1080 screen inside the scanner, and participants indicated their responses using a button box, with one finger from each hand in tasks that had two-choice decisions (all tasks except autobiographical memory).

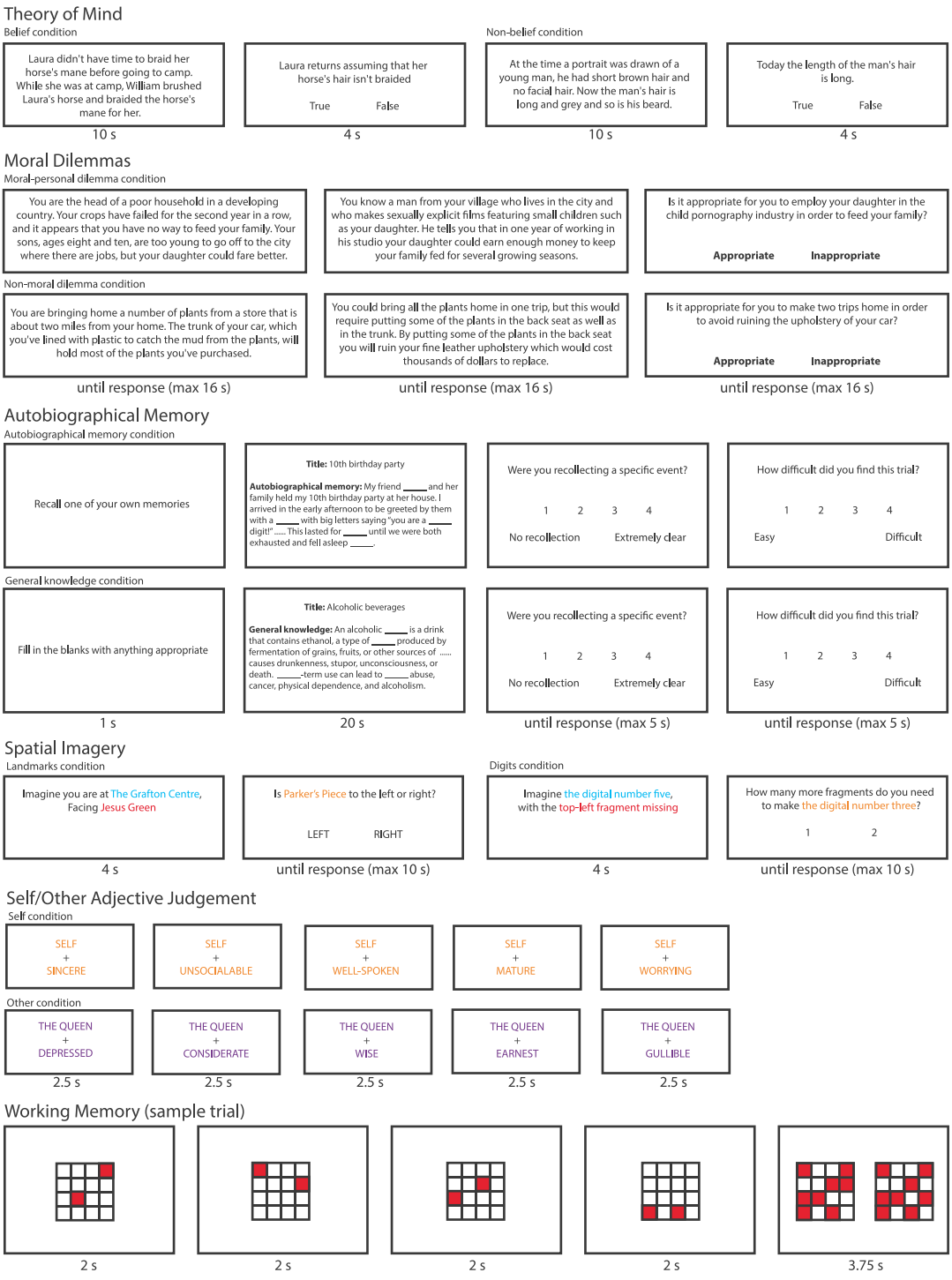

Figure 1. Example trial/block from each of the six tasks: theory of mind, moral dilemmas, autobiographical memory, spatial imagery, self/other adjective judgment, and working memory. All stimuli were shown on a 1920 × 1080 screen (stimulus size and width/height ratio has been adjusted for this figure for illustration purposes). The examples in the autobiographical memory task were shortened to fit in the figure.

According to Andrews-Hanna (2012), the chosen tasks would be hypothesized to differently engage the dMPFC and MTL subsystems, with all tasks engaging the core hubs. The theory of mind and moral dilemmas tasks were chosen as tasks requiring "introspection about mental states" and were hypothesized to recruit the dmPFC subsystem. The autobiographical memory and spatial imagery tasks were chosen as tasks that required "memory-based construction/simulation" and were hypothesized to recruit the MTL subsystem. The self/other judgment task was chosen as a task that involved "personally significant information", and was hypothesized to recruit predominantly the core hubs. Finally, the working memory task was chosen to

examine the activity of the DMN during passive rest compared to an external task. We note that, although we selected six distinct tasks, with as little overlap as possible, it is possible that some cognitive processes may be common across tasks. For example, research has shown that participants prefer to recall autobiographical memories involving social experiences (Speer and Delgado 2019), which may activate the dMPFC subsystem in addition to the MTL subsystem.

Theory of Mind Task

The theory of mind task was adapted from Dodell-Feder et al. (2011). On each trial, participants were presented with a short story to read for 10 seconds. Afterwards participants were given a statement related to the story and were asked to judge whether it was "true" or "false" by pressing a button (left or right). Some trials involved making judgments about other people's beliefs, while others involved making nonbelief judgments. Each question stayed on the screen up to 10 seconds, or until the participant made a button press. This was then followed by a 10–24-second fixation period before the next trial began. Each run consisted of five trials of each condition (belief and nonbelief).

Moral Dilemmas Task

The moral dilemmas task was adapted from Greene et al. (2001). On every trial, participants were presented with a hypothetical situation that posed a dilemma that could either be a moral-personal dilemma (MPD) or a nonmoral dilemma (NMD). Each dilemma was presented as text through a series of three displays, with the first two describing a scenario and the third posing a question about the appropriateness of an action one might perform in such a situation. The maximum time one display could be on screen was 16 seconds, but when participants finished reading the text, they were allowed to press any button to move on to the next display. On the third display, participants made the appropriateness judgment by pressing a button (left or right). They were told that there was no correct answer for many of the questions, and were asked to consider each situation carefully and provide their best answer. A 6–8-second fixation cross was presented in between each trial. Each run consisted of five trials of each condition (MPD or an NMD).

Autobiographical Memory Task

Prior to the experiment, participants were asked to provide 12 written personal memories, each with a title that provided a general description of its contents. Participants were given specific instructions to provide clear memories, where they were able to remember the people, objects, and location details featured in the corresponding memory. Each memory was required to be between 100 and 150 words long. All events were required to be temporally and contextually specific, occurring over minutes or hours, but not more than 1 day. The memories were then edited by the experimenter such that 13–17 critical words were removed and replaced with a blank underscore line. Occasionally, if the memories participants sent were too long, they were shortened; or if the memories were too short or contained too few details, a new sentence with a prompt was added (e.g., "I was wearing a _____", "It was around _____ o'clock", "I felt very _____").

During the task, on a given trial, participants were given a 100–150-word long text to read with 13–17 critical words missing, and were asked to fill in the blanks in their mind. Half of the trials used text adapted from the participants' autobiographical memories; the other half contained text related to general knowledge (either procedural tasks, such as "how to make chocolate chip cookies", or knowledge about a common topic, such as "alcoholic beverages"). Before the onset of the text display, a 1-second cue was presented to indicate the upcoming condition. For autobiographical memory trials, participants were told to try to "really get into the memory" while filling in the blanks. They were asked to try to imagine themselves reliving that experience. In the general knowledge condition, participants were asked to fill in the blanks with anything appropriate, and to try to "think carefully for good answers". All trials were terminated after 20 seconds. However, participants were told that there was no need to rush to try to finish all the blanks, and it was more important to be accurate than fast. This was designed to encourage participants to be engaged as much as possible throughout the 20 seconds. After the 20 seconds were over, participants were given two rating questions ("Were you recollecting a specific event?" and "How difficult did you find this trial?"). They were given 5 seconds to provide each rating on a scale of 1 to 4. Since it involved four buttons, participants gave responses with the four fingers of their right hand. This was then followed by an 8–12-second fixation period between trials. There were five trials of each condition (autobiographical memory and general knowledge) in each run.

Spatial Imagery Task

In the spatial imagery task, there were two types of mental imagery conditions, each presented in blocks of trials. One type of block involved judging relative locations of landmarks in Cambridge (this task was adapted from Vass and Epstein 2017). On each trial, there was first a 4-second instruction to imagine standing at the landmark indicated in the first line (e.g., Botanic Garden) while facing the landmark indicated in the second line (e.g., King's College). Afterwards, participants were shown a second screen with a new landmark location (e.g., Parker's Piece), and were asked to indicate whether it would be on their left or right (in this example the correct answer would be right). The question stayed on the screen for up to 10 seconds, or until participants made a button press. The other type of block involved judging how many fragments were needed to complete a target digital number. At the beginning of each trial, a 4-second instruction was given to imagine a digital number indicated in the first line (e.g., three) with either an additional fragment or a fragment missing indicated in the second line (e.g., top-right fragment missing). Afterwards, participants were shown a new screen indicating a new target digit (e.g., five), and were asked how many more fragments would need to be added to their original mental image to complete the target (in this example, the correct answer would be one). Participants had up to 10 seconds to answer one or two (left and right buttons). The two conditions (landmarks and digits) were presented in blocks of four trials, with a 6–16-second fixation period in between each block. There were four blocks of each condition per run.

Self/Other Adjective Judgment Task

The self/other judgment task was adapted from Kelley et al. (2002). A total of 160 adjectives were selected from a pool of normalized personality trait adjectives (Anderson 1968). Half of the words were positive traits and half were negative. On each trial, participants were asked to make a yes/no judgment via button press to indicate whether an adjective shown on the

bottom of the screen described the person indicated on the top of the screen (self or the Queen). Each trial was presented for a fixed period of 2 seconds followed by a 0.5-second fixation. The task was grouped into blocks according to "self" and "the Queen", with each block consisting of five trials. There were eight blocks of each condition per run. A 6–16-second fixation period separated each block.

Working Memory Task

The working memory task was adapted from Fedorenko et al. (2013). On each trial, participants were presented with four consecutive displays. Each display was a 4×4 grid, with two of the cells colored red and the remaining white. Each display was presented for 2 seconds. Afterwards, participants were presented with two choice displays, on the left and right of the screen, one of which had eight red cells in locations corresponding to those from the previous four displays, while the other was similar but with one cell misplaced. Participants were given 3.75 seconds to indicate the correct display by pressing left or right. This was followed by a 0.25-second feedback on the accuracy of their choice. There was a 12–16-second fixation period between trials. Each run consisted of 16 trials.

fMRI Data Acquisition and Preprocessing

Scanning took place in a 3T Siemens Prisma scanner with a 32-channel head coil. Functional images were acquired using a standard gradient-echo echo-planar imaging (EPI) pulse sequence (TR = 2000 ms, TE = 30 ms, flip angle = 78°, 64×64 matrices, slice thickness = 3 mm, 25% slice gap, voxel size $3 \times 3 \times 3$ mm, 32 axial slices covering the entire brain). The first five volumes served as dummy scans and were discarded to avoid T1 equilibrium effects. Field maps were collected at the end of the experiment (TR = 400 ms, TE = 5.19 ms/7.65 ms, flip angle = 60°, 64×64 matrices, slice thickness = 3 mm, 25% gap, resolution 3 mm isotropic, 32 axial slices). High-resolution anatomical T1-weighted images were acquired for each participant using a 3D MPRAGE sequence (192 axial slices, TR = 2250 ms, TI = 900 ms, TE = 2.99 ms, flip angle = 9°, field of view = $256 \times 240 \times 160$ mm, matrix dimensions = $256 \times 240 \times 160$, 1 mm isotropic resolution).

The data were preprocessed and analyzed using automatic analysis pipelines and modules (Cusack et al. 2015), which called relevant functions from Statistical Parametric Mapping software (SPM 12, http://www.fil.ion.ucl.ac.uk/spm) implemented in Matlab (The MathWorks, Inc., Natick, MA, USA). EPI images were realigned to correct for head motion using rigid-body transformation, unwarped based on the field maps to correct for voxel displacement due to magnetic field inhomogeneity, and slice-time corrected. The T1 image was coregistered to the mean EPI, and then coregistered and normalized to the MNI template. The normalization parameters of the T1 image were applied to all functional volumes. Spatial smoothing of 10 mm FWHM was applied for whole-brain univariate second-level analysis, but no smoothing was applied for ROI-based analyses or multivoxel pattern analysis.

A general linear model was estimated per participant and per voxel for each of the six tasks. A high-pass filter with 1/128 Hz cutoff was applied to both the data and the model. For the first five tasks, regressors were created for each condition, with fixation periods serving as implicit baseline. In the working memory task, one regressor was created for the fixation periods to model passive fixation as the contrast against active task as implicit baseline. Error trials (only applicable for the theory of mind and spatial imagery tasks) and no-response trials were modeled using a separate regressor and discarded. All regressors were created by convolving the interval between stimulus onset and response (or display offset when no responses were required) with the canonical hemodynamic response function. Run means and movement parameters were included as covariates of no interest. The resulting beta estimates were used to construct contrasts between the two conditions of each task, or for working memory, the contrast of rest against task as implicit baseline.

Whole-Brain Univariate Analysis

The between-condition contrasts that were used to examine DMN activity were: 1) belief > nonbelief in the theory of mind task; 2) MPD > NMD in the moral dilemmas task; 3) autobiographical memory > general knowledge in the autobiographical memory task; 4) landmarks > digits in the spatial imagery task; 5) self > other in the self/other adjective judgment task; and 6) rest > working memory.

A second-level whole-brain analysis (one-sample *t*-test across subjects) was conducted on each of the six within-subject contrasts above, to obtain group activation maps for each contrast separately. Activation maps were thresholded at $P < 0.05$, controlling the false discovery rate (FDR; Benjamini and Yekutieli 2001). In addition, a whole-brain analysis was conducted to examine individual participant activations for each of the six contrasts. For each voxel, we computed the number of participants with significant activation, applying FDR correction across all voxels of all participants (Heller et al. 2007). This resulted in a whole-brain map showing the number of participants with significant activation within each voxel. Based on the six random effects analyses mentioned above, a similar map was constructed to show the number of significant task contrasts at each voxel (Heller et al. 2007). MRIcroN (Rorden et al. 2007) was used for visualization of whole-brain maps.

Regions of Interest and ROI Analysis

A DMN mask was constructed using the 17 network parcellation from Yeo et al. (2011), concatenating networks 10, 15, 16, and 17. Networks 15, 16, and 17 largely corresponded to the three DMN subnetworks described in Andrews-Hanna (2012), which are the MTL subsystem, the dmPFC subsystem, and the core hubs. Network 10 was described in Yeo et al. (2011) as the orbital frontal–temporopolar network that consists of temporopolar and orbital frontal regions. This network was added to the three DMN networks from Yeo et al. (2011) to include the vmPFC region described by Andrews-Hanna (2010). To create a single symmetrical volume, ROI masks (1 for voxels within the region; 0 outside) from the left and right hemispheres were combined using a logical OR operation, then projected back to both hemispheres. The combined network was then slightly smoothed (4 mm FWHM), and voxels with values >0.5 after smoothing were retained. Finally, the combined network was parcellated into 20 smaller subregions by assigning each voxel to its closest DMN coordinate described by Andrews-Hanna et al. (2010). The coordinates are listed in Table 1. In cases where noncontiguous volumes were assigned to the same region, any volumes of <45 voxels were discarded, and the remaining volume with center of mass closest to the Andrews-Hanna coordinate was chosen. The number of voxels for each ROI ranged from 219 to 7952 (mean = 1552). The resulting ROIs are shown in Figure 2.

Table 1 Characteristics of DMN ROIs used in the study. DMN coordinates described in Andrews-Hanna et al. (2010) were used to parcellate the Yeo networks corresponding to the DMN

Region	Abbreviation	x	y	z	# of voxels
dMPFC subsystem					
Dorsal medial prefrontal cortex	dMPFC	0	52	26	7952
Temporal parietal junction	TPJ	−/+54	−54	28	1079
Lateral temporal cortex	LTC	−/+60	−24	−18	1784
Temporal pole	TempP	−/+50	14	−40	835
MTL subsystem					
Ventral medial prefrontal cortex	vMPFC	0	26	−18	3538
Posterior inferior parietal lobule	pIPL	−/+44	−74	32	993
Retrosplenial cortex	Rsp	−/+14	−52	8	326/315
Parahippocampal cortex	PHC	−/+28	−40	−12	825
Hippocampal formation	HF+	−/+22	−20	−26	219
Core hubs					
Anterior medial prefrontal cortex	aMPFC	−/+6	52	−2	2879/2568
Posterior cingulate cortex	PCC	−/+8	−56	26	1677/1393

Note: Coordinates are based on the Montreal Neurological Institute coordinate system.

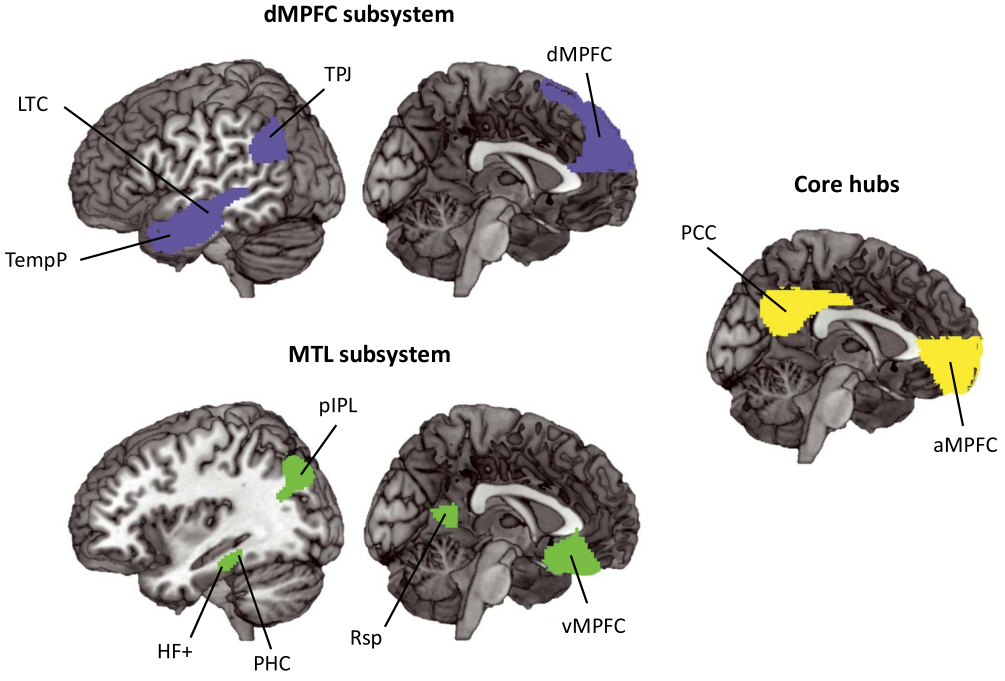

Figure 2. DMN ROIs used in the current experiment. The ROIs are derived from networks 10, 15, 16, and 17 described in the 17 network parcellation in Yeo et al. (2011) and divided according to coordinates described in Andrews-Hanna et al. (2010). Regions in blue are part of the dMPFC subsystem, and include the midline dMPFC and bilateral TPJ, LTC, and TempP. Regions in green are part of the MTL subsystem, and include the midline vMPFC and bilateral pIPL, Rsp, PHC, and HF+. The core hubs are represented in yellow, and include the bilateral aMPFC and PCC. For abbreviations, see Table 1.

To corroborate our findings with ROIs based more closely on the original coordinates of Andrews-Hanna et al. (2010), we created 10 mm spheres centered on these coordinates and repeated the same analyses. One participant did not have any signal in their right TempP, and it was removed from the analyses.

For each task, the contrast between the two conditions was averaged within each ROI using the MarsBAR toolbox (Brett et al. 2002). For working memory, the relevant contrast was simply rest against implicit baseline (active task). Contrasts were tested against zero using two-tailed *t*-tests across subjects, corrected using FDR < 0.05 for multiple comparisons across ROIs. ROI $\times$ task ANOVAs were used to examine differences in ROI activity across different contrasts. Finally, for each ROI, data averaged across participants were used to construct a mean activation profile, i.e., a vector of contrast values from the six tasks. Distances between activation profiles for each pair of ROIs were calculated using 1 − Pearson's r, and classical multidimensional scaling (MDS) was used to visualize the differences in activation pattern between ROIs as two-dimensional distances.

Task-Wise Multivoxel Pattern Similarity

For each ROI, we wished to examine similarity of voxelwise activity patterns across the six tasks. For each participant, we extracted the beta values for each contrast for each task, and compared the multivoxel patterns of these values between tasks. The similarity between each pair of tasks

was measured by Pearson's *r*, producing a symmetrical 6 × 6 matrix of similarities for each ROI for each participant. The similarity matrices were then rank transformed. For each ROI, we quantified which regions showed 1) greater pattern similarity between the two tasks that required "introspection about mental states" (theory of mind and moral dilemmas), compared to similarity of these tasks to others, 2) greater pattern similarity between the two tasks that required "memory-based construction/simulation" (autobiographical memory and spatial imagery), compared to similarity of these tasks to others, 3) a relatively unique pattern for the self/other judgment task (greater similarity for task pairs not including self/other), and 4) a relatively unique pattern for rest (greater similarity for task pairs not including rest). To do this, we created four model similarity matrices based on these a priori groupings and evaluated fits to each ROI's task similarity matrix using Kendall's tau-a for each participant, as recommended when the model similarity matrix has ties (Nili et al. 2014). Tau-a correlations were tested against zero using two-tailed *t*-tests across participants, and all tests were corrected for multiple comparisons (FDR < 0.05) across the number of ROIs and models.

To compare patterns of task similarities between ROIs, we used vectors of between-task correlation from the above analysis (15 between-task correlations for each ROI, rank transformed for each participant and averaged across participants). Similarly to the univariate analysis, distances between each pair of ROIs were calculated using 1 minus the correlation (Pearson's *r*) between these vectors. Again, classical MDS was used for visualization.

Results

Behavioral Results

Mean reaction times (RTs) for all responses are summarized in Table 2. The first three subjects' RTs for the working memory task were not recorded due to technical error and were excluded in the analysis. Mean accuracies for the theory of mind, spatial imagery, and working memory tasks are also summarized in Table 2, along with mean ratings of recollection and difficulty for the autobiographical memory task.

Paired *t*-tests were conducted between the two conditions of the first five tasks, with no correction for multiple comparisons, to examine how well matched each of the two conditions were within a task. There were no differences in RT between the pairs of conditions in the theory of mind, moral dilemmas, autobiographical memory, and self/other adjective judgment task (all |t|s < 1.45, all Ps > = 0.16). In the spatial imagery task, RTs were shorter for the landmarks condition than for the digits condition ($t = -2.74$, $P = 0.01$). There were no differences in accuracy between the pairs of conditions in the theory of mind and spatial imagery task (both |t|s < 1.62, both Ps > = 0.12). As expected, ratings of recollection were significantly greater in the autobiographical memory condition than in the general knowledge condition ($t = 21.01$, $P < 0.001$); autobiographical memory was also rated less difficult than general knowledge ($t = -4.47$, $P = 0.001$).

Table 2 RTs, accuracies, and ratings of each condition (mean ± standard error)

	Theory of Mind		Moral dilemmas		Autobiographical memory		Spatial imagery		Self/other adjective judgment		Working memory
	Belief	Nonbelief	MPD	NMD	Memory	Knowledge	Landmarks	Digits	Self	Other	
RT (s)	3.24 ± 0.03	3.10 ± 0.02	3.50 ± 0.03	3.26 ± 0.04	1.84 ± 0.02	1.90 ± 0.02	2.30 ± 0.02	3.02 ± 0.05	1.44 ± 0.01	1.47 ± 0.01	1.84 ± 0.02
Accuracy (% correct)	87.4 ± 6.2	91.1 ± 4.7	N/A	N/A	N/A	N/A	91.7 ± 5.7	84.3 ± 8.6	N/A	N/A	76.4 ± 5.0
Rating	N/A	N/A	N/A	N/A	Recollection 3.65 ± 0.02 Difficulty 1.41 ± 0.02	Recollection 1.36 ± 0.01 Difficulty 1.91 ± 0.02	N/A	N/A	N/A	N/A	N/A

Whole-Brain Univariate Analysis

A whole-brain random effects analysis was conducted separately for each of the six contrasts of interest (Fig. 3A; belief > nonbelief; MPD > NMD; autobiographical memory > general

knowledge; landmarks > digits; self > other; and rest > task). Consistent with previous findings, the group analysis revealed many regions that are commonly associated with the DMN. In most tasks, we see activation in the medial prefrontal cortex (MPFC) and posterior medial cortex including PCC, precuneus, and Rsp, as well as temporal and parietal regions on the lateral surface, including pIPL, TPJ, and LTC. Activity for the self/other adjective judgment task was less typical of the DMN, though strong in a large portion of the MPFC.

To further quantify consistency across subjects, we computed a whole-brain overlay map for each task, where warmer colors indicate greater number of participants with significant activations (Fig. 3B). The subject overlay map is largely consistent with the random effects results, as expected, but also indicates variability across participants.

Next, we identified regions that were consistently significantly activated across multiple contrasts (Fig. 3C). No region was found to be active in all six contrasts after correcting for multiple comparisons (FDR < 0.05). However, several regions showed significant involvement in at least five contrasts. These include the MPFC (including dMPFC, aMPFC, and vMPFC), PCC, pIPL, TPJ, and parts of the LTC.

The results show that all six manipulations activated much of the DMN, and in particular, voxels within the MPFC, PCC, pIPL, TPJ, and LTC were significantly active for at least five manipulations. The theory of mind and moral dilemmas tasks showed strong activation of dMFPC, while the autobiographical memory and spatial imagery tasks showed peaks in vMPFC. These differences correspond to Andrews-Hanna's (2012) observation of the dMPFC being involved in "introspection about mental states" and the vMPFC being involved in "memory-based construction/simulation". Furthermore, the theory of mind and moral dilemmas tasks activated more anterior portions of the IPL than the autobiographical memory and spatial imagery tasks. This again corresponds to the separation of the TPJ (more anterior) and pIPL (more posterior) regions of the IPL, and matches their assignment to the dMPFC and MTL subsystems. The self > other contrast most consistently activated the MPFC across subjects, one of the core hubs identified by Andrews-Hanna (2012) to be responsive to "personally significant information". However, the other hub region, the PCC, was only weakly activated. Our results show activity across much of the DMN for multiple contrasts, along with a degree of differentiation between dMPFC and MTL subsystems.

ROI Analysis of Univariate Activation Level

For each of our six contrasts, profiles of activity across DMN ROIs are shown in Figure 4A(1). All contrasts were compared against zero using *t*-tests and were corrected for multiple comparisons with FDR < 0.05.

Examined in detail, profiles suggest some of the anticipated differences between DMN regions, but also some surprises. As expected, theory of mind and moral dilemmas showed significant effects in most regions of the dMPFC and core networks. Activations were also seen in some regions of the MTL subsystem, however, including vMPFC, pIPL, and PHC. Averaged contrasts within each network (Fig. 4A(2)) showed significant effects just for the dMPFC subsystem and core. As anticipated, autobiographical memory and spatial imagery showed strong effects in the MTL subsystem, especially Rsp, and again in the core hubs, but significant effects were also seen in most dMPFC regions. Averaged within subsystems, the response of dMPFC was significantly lower than the other subsystems, but significantly greater than zero. For self–other, activations were more restricted, but included all three regions of the MPFC. Averaged within networks, this contrast was significant in the core and dMPFC subsystem, and, again as anticipated, strongest in the core subsystem. Unlike the previous four contrasts, core activation for self/other was stronger in aMPFC than in PCC. Perhaps surprisingly, the contrast of rest with working memory showed rather weak activations, significant only in the core and dMPFC subsystem, and significantly negative for some regions of the MTL network.

Overall, these results provide partial support for the division into three subsystems, with the dMPFC subsystem especially involved in "introspection about mental states", the MTL subsystem especially involved in "memory-based construction/simulation", and the core hubs involved in all tasks including sensitivity to "personally significant information". At the same time, the results show that separation of networks is far from complete, with at least part of each network activated by every contrast. Within each network, there are also some clear variations in response. Notably, within the MTL subsystem, activity in the Rsp, PHC, and HF+ was almost entirely restricted to autobiographical memory and spatial imagery; the pIPL and vMPFC, in contrast, were active for five of the six tasks, similar to the core hubs and dMPFC subsystem. Within the core, aMPFC showed especially strong sensitivity to self/other, while several other contrasts more strongly drove PCC.

To compare profiles statistically, the data were entered into a repeated measures ROI (20) × task (6) ANOVA. Consistent with the different profiles suggested by Figure 4A(1), there was a strong interaction between ROI and task ($F(95,2470) = 55.57$, $P < 0.001$). There were also significant main effects for task ($F(5,130) = 46.66$, $P < 0.001$) and ROI ($F(19,494) = 25.61$, $P < 0.001$). The interaction in part reflects differences between the three subsystems, so we next repeated the ANOVA using the subsystem average profiles shown in Figure 4A(2). The significant interaction ($F(10,260) = 100.05$, $P < 0.001$) confirms that this subnetwork grouping captures different functional profiles across the tasks. There were also main effects for networks ($F(2,52) = 15.09$, $P < 0.001$) and task ($F(5,130) = 35.01$, $P < 0.001$). We also wished to test for possible heterogeneity within each subsystem. To this end, ROI × task ANOVAs were repeated for each network separately. For the dMPFC subsystem, there was a significant interaction between ROI and task ($F(30,780) = 9.21$, $P < 0.001$), as well as main effects for ROI ($F(6,156) = 27.54$, $P < 0.001$) and task ($F(5,130) = 12.50$, $P < 0.001$). For the MTL subsystem, we also observed a significant interaction between ROI and task ($F(40,1000) = 34.15$, $P < 0.001$), as well as main effects for ROI ($F(8,208) = 29.78$, $P < 0.001$) and task ($F(5,130) = 110.86$, $P < 0.001$). Finally, there was also a significant interaction ($F(15,390) = 22.92$, $P < 0.001$) as well as main effects of ROI ($F(3,78) = 25.42$, $P < 0.001$) and task ($F(5,130) = 12.87$, $P < 0.001$) in the core hubs. This suggests a hierarchical picture, with functional divisions within, as well as between, subsystems.

The dissimilarity between activation profiles for each pair of ROIs (each ROI a vector of 6 contrasts) was calculated using 1 − Pearson's *r* (see Methods). The resulting distance matrix (Fig. 4B), based on the dissimilarity of activation profiles for the 20 ROIs, showed distinct clusters. Profiles were largely similar for all regions in the dMPFC subsystem (Fig. 4B, upper left), although dMPFC itself was somewhat separated from the cluster, being displaced toward aMPFC. In addition, the activation profile for left LTC resembled the MTL as well as the other regions in

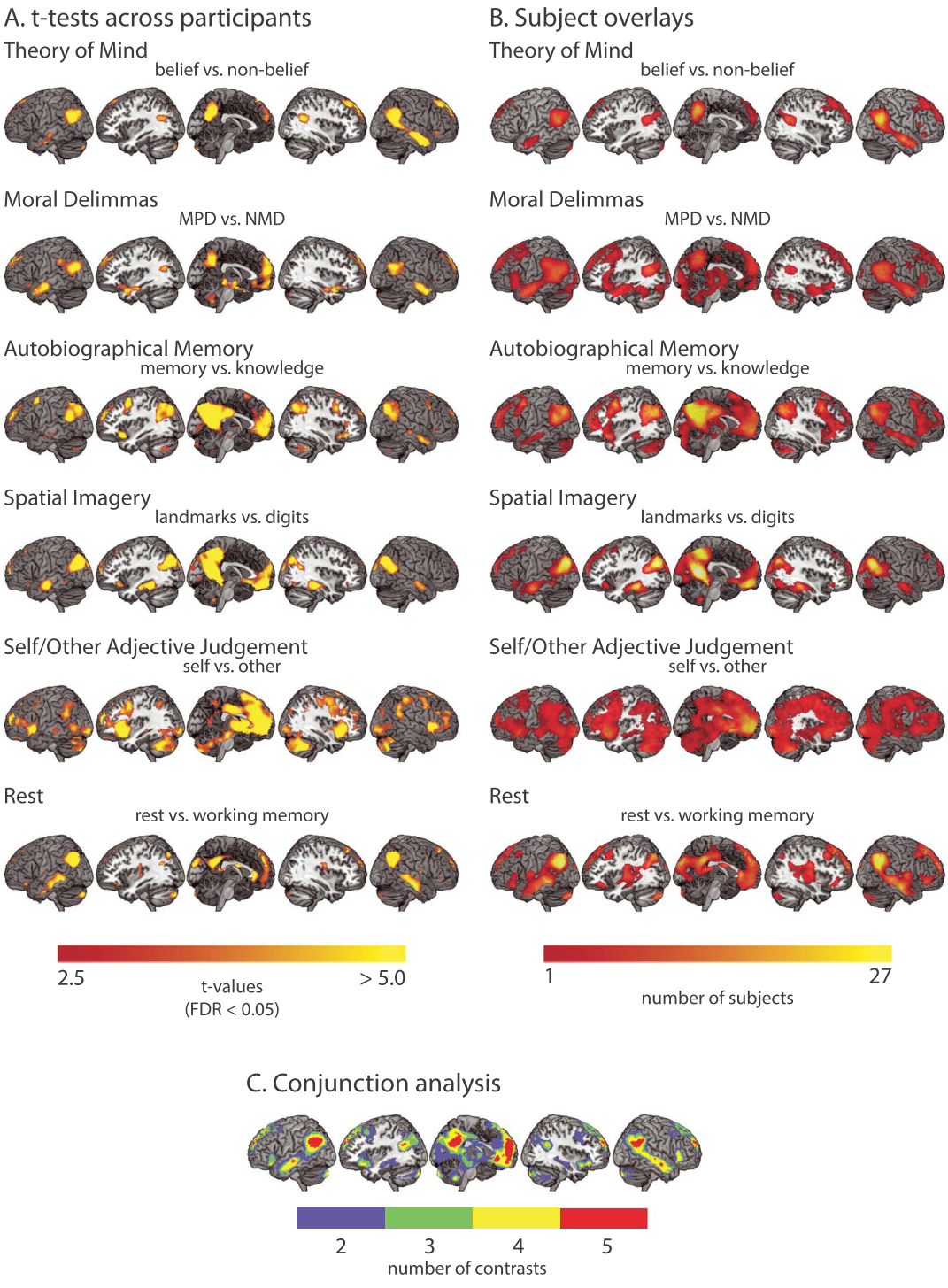

Figure 3. Univariate activity showing recruitment of the DMN network by all six tasks. (*A*) Whole-brain *t*-maps of the contrasts of interest in the six tasks. This includes belief > nonbelief in the theory of mind task; MPD > NMD in the moral dilemmas task; autobiographical memory > general knowledge in the autobiographical memory task; landmarks > digits in the spatial imagery task; self > other in the self/other adjective judgment task; and rest > working memory in the working memory task. *t*-maps were thresholded at $P < 0.05$ (FDR corrected). (*B*) Overlay map of significant activations found in single subjects in the contrasts of interest. The color of each voxel represents the number of subjects that had significant activation in that voxel for a particular contrast, thresholded at one subject. (*C*) Overlay map of the number of significant contrasts from the six second-level analyses. The color of each voxel represents the number of contrasts that had significant activation in that voxel, thresholded at two contrasts.

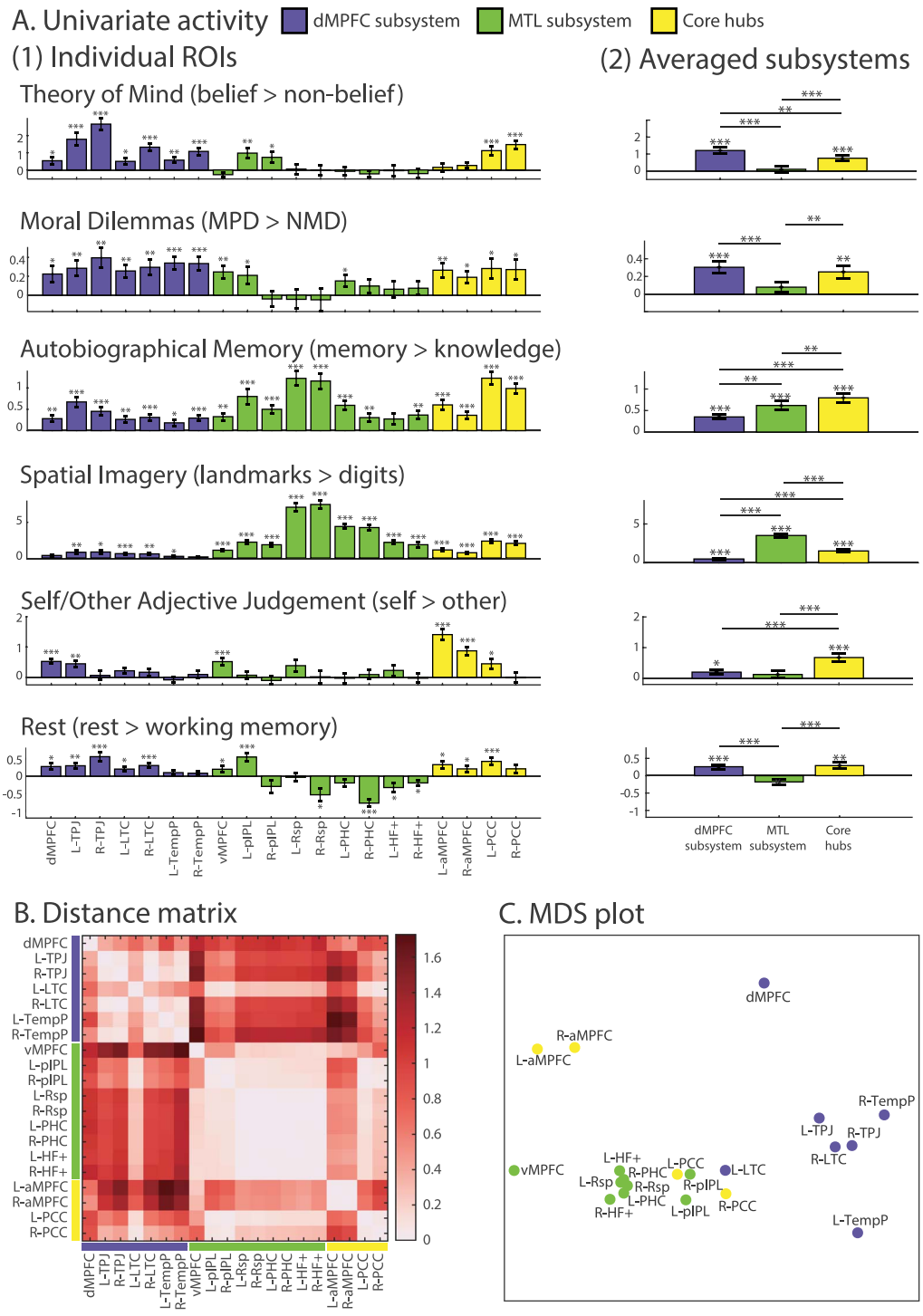

Figure 4. (*A*) Activity (difference in beta) for each task contrast, for individual ROIs (1) and averaged over ROIs in each subsystem (2). Error bars represent standard error. *t*-tests against zero were conducted for each contrast. *** indicates $P < 0.001$, ** indicates $P < 0.01$, and * indicates $P < 0.05$ (all tests were corrected for multiple comparisons using FDR). Note that scales differ for different contrasts. (*B*) Dissimilarity matrix calculated using 1 − Pearson's *r* between ROIs based on their activity profile across the six tasks. (*C*) MDS to visualize the dissimilarity between regions. L- and R- indicate left and right.

the dMPFC subsystems. Regions in the MTL network also had largely similar profiles (Fig. 4B, middle), but with other notable features. vMPFC resembled not only other MTL regions, but also aMPFC, while for pIPL, there was high similarity not only to other MTL regions, but also to much of the dMPFC subsystem and conspicuously also to PCC. Within the core regions, aMPFC had a relatively distinct profile, but was most similar to other frontal regions, while PCC instead showed results closely similar to those of pIPL, with similarity to all other regions except for aMPFC, dMPFC, and TempP.

The results of Figure 4B are visualized using the MDS plot shown in Figure 4C. As expected, regions of the dMPFC network largely cluster together, but with dMPFC shifted toward other frontal regions. Regions of the MTL network are again close together, with vMPFC somewhat apart from the main cluster. PCC, instead of clustering with its partner core region, is placed between dMPFC and MTL networks, in a position close to pIPL. aMPFC occupies a position between the other two frontal regions, as perhaps expected from anatomical proximity.

Analyses using spherical ROIs derived from the coordinates in Andrews-Hanna et al. (2010) showed largely similar results, though activations for LTC were less robust, while the response profiles of vMPFC and dMPFC fell closer to their subsystem clusters (see Supplementary Fig. 1).

For completeness, for the five tasks except working memory, Supplementary Figure 2 shows contrasts of each condition against rest (implicit baseline). For the dMPFC subsystem, significant contrasts in the main analysis mainly resulted from positive activation against rest for the "active" condition. In the MTL subsystem, this was also true for autobiographical memory and spatial imagery tasks. In the core, results were mixed for the PCC, and intriguingly, aMPFC was largely deactivated compared to rest.

Task-Wise Multivoxel Pattern Similarity

For each ROI, we moved on to assess the similarity of voxel-wise activity patterns across our six task contrasts. For each participant, voxelwise patterns for the six contrasts were correlated with one another, producing a 6×6 matrix of task similarities for each ROI, which were then rank transformed. Mean ranks across participants are shown in Figure 5A(1) (leftmost section for each ROI). Four model similarity matrices were constructed to test 1) whether the two "introspection of mental states" tasks were especially similar, 2) whether the two "memory-based construction/simulation" tasks were especially similar, 3) whether the self/other adjective judgment task was especially dissimilar to other contrasts, and 4) whether rest > working memory was especially dissimilar to other contrasts. Data for each participant were correlated (Kendall's tau-a) with the four model matrices, and correlations tested against zero using a *t*-test across participants (see Methods). Results (Fig. 5A(1), rightmost section for each ROI) showed that the dMPFC subsystem, especially in the right hemisphere (dMPFC, right TPJ, right LTC, and right TempP), as well as pIPL and PCC, had strong pattern similarity between the two "introspection" tasks (Model 1). The MTL subsystem (pIPL, Rsp, PHC, and HF+), as well as aMPFC and PCC, showed strong pattern similarity between the two "memory-based construction" tasks (Model 2). Across many ROIs of the three subsystems there was a strong tendency for the self > other pattern to be distinct from others (Model 3; greater similarity for contrast pairs not involving self/other). Few regions, however, showed the rest > working memory pattern to be distinct from the others (Model 4; only right Rsp). Results averaged over ROIs within each subnetwork are shown in Figure 5A(2). Together, these data complement the findings in Figure 4. Though regions in each subsystem contain voxels responding to each contrast, the pattern of these activations is organized along the lines proposed by Andrews-Hanna (2012), with more dissimilar activation patterns for contrasts predominantly associated with different networks.

In a final analysis we wished to assess similarity of ROIs in terms of their pattern of multivoxel task discrimination. For each ROI, the above analysis produced a vector of 15 between-task correlations, rank transformed for each participant and then averaged across participants. For each pair of ROIs, we correlated these vectors and expressed dissimilarity as 1 − Pearson's *r*. The resulting distance matrix (Fig. 5B) and MDS plot (Fig. 5C) showed distinct clusters, largely similar to those based on univariate activity profiles. The ROIs of the dMPFC subsystem clustered with each other, as did many of the MTL ROIs. Again, however, PCC and IPL regions clustered close together, between dMPFC and MTL clusters, and again, despite putative assignment to different networks, there was some similarity of the three MPFC regions.

Analyses using spherical ROIs derived from the coordinates in Andrews-Hanna et al. (2010) showed similar results (see Supplementary Fig. 3). Again, the MDS plot showed broad separation of dMPFC and MTL subsystems, with PCC and pIPL lying between the two, and MPFC regions lying somewhat to one side of the remainder.

Discussion

Many complex cognitive processes have been linked to the DMN, supporting its role in high-level thought (Buckner and Carroll 2007; Buckner et al. 2008; Spreng et al. 2009; Andrews-Hanna 2012; Andrews-Hanna et al. 2014b). Among the most established of these cognitive functions are social, semantic, episodic, and self-relevant processing (Frith and Frith 2006; Binder et al. 2009; McDermott et al. 2009; Spreng et al. 2009; Humphreys and Lambon Ralph 2017). Recent findings suggest that the DMN consists of anatomically and functionally heterogeneous subsystems (Yeo et al. 2011; Andrews-Hanna 2012; Andrews-Hanna et al. 2014b; Axelrod et al. 2017; Braga & Buckner, 2017). Here, we used six diverse tasks to examine functional similarities and differences between DMN regions, guided by the proposed tripartite split into dMPFC, MTL, and core subsystems (Andrews-Hanna et al. 2010; Andrews-Hanna 2012; Andrews-Hanna et al. 2014b).

Our results were largely in accord with predictions for the dMPFC subsystem. In terms of univariate activity, regions of this subsystem had largely similar activity profiles (Fig. 4A, B), with strong response to our two social tasks, consistent with a particular role in social cognition or introspection about mental states. A partial exception was dMPFC itself, whose activity profile was shifted toward that of aMPFC (Fig. 4B, C). In addition to their strong response to social contrasts, however, dMPFC regions also showed some response to most other contrasts (Fig. 4A). Thus, specialization was quantitative rather than qualitative. Analysis of multivoxel activity patterns also largely supported the concept of a dMPFC subsystem, with regions of this subsystem showing similar voxelwise activity patterns for our two social contrasts (Fig. 5A), and again, largely similar profiles of between-task distances (Fig. 5B, C).

Our results also support the proposal of an MTL subsystem, though with some caveats. In terms of univariate activity, regions of the MTL subsystem had largely similar activity profiles (Fig. 4A, B), with especially strong response to the autobiographical memory and spatial imagery tasks. For posterior medial structures (Rsp, PHC, and HF+), indeed, there was little response to other contrasts (Fig. 4A), suggesting that these regions form an especially dedicated subsystem underlying memory-based construction/simulation. While other regions of the MTL subsystem (vMPFC and pIPL) somewhat resembled these posterior medial regions, there were also clear

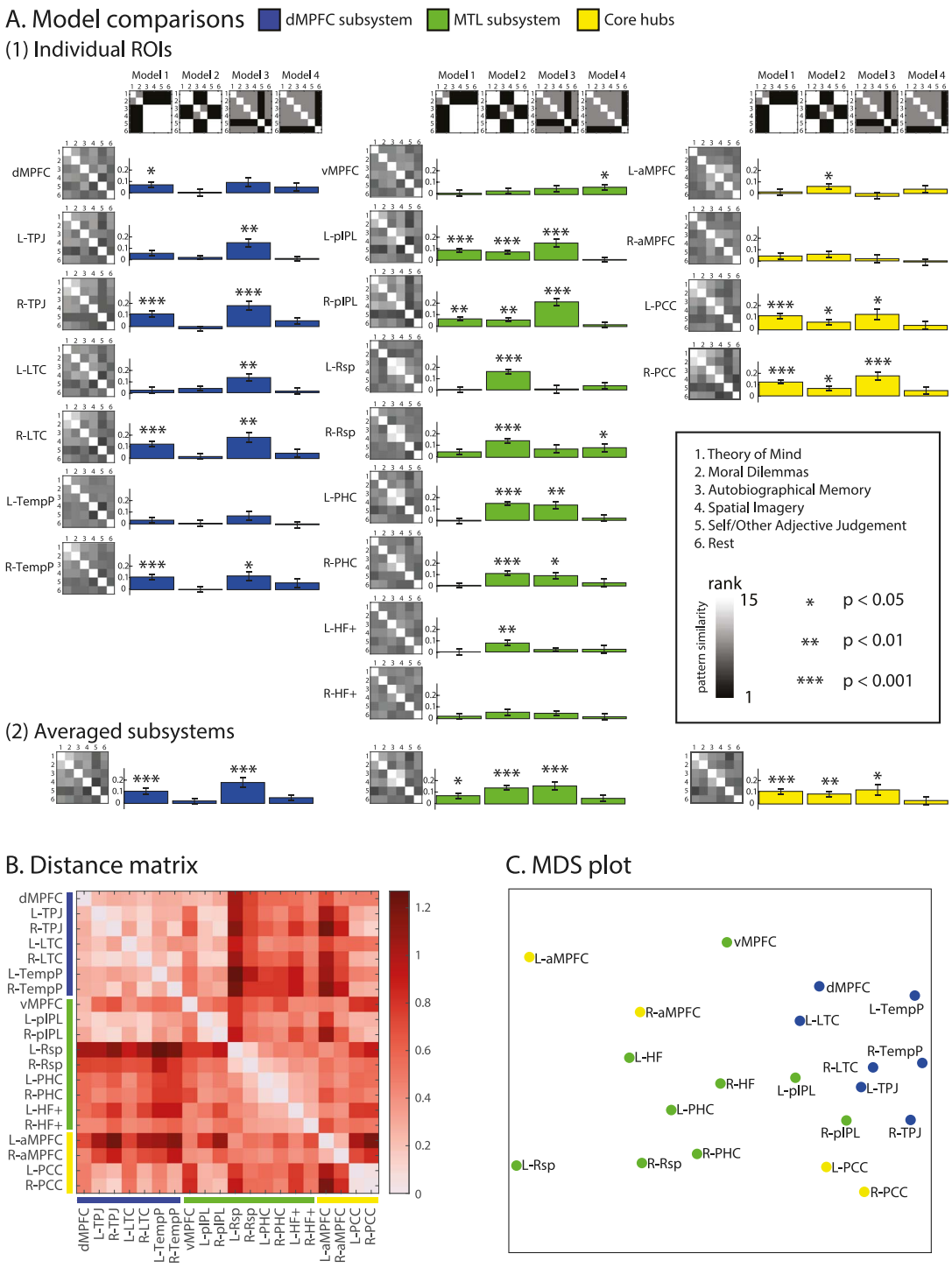

Figure 5. (A) (1) Similarity of multivoxel patterns for the six tasks, shown separately for each ROI (top to bottom in each column) in each subsystem (left, center, and right columns). For each ROI, the leftmost image shows the rank-transformed similarity matrix, separately calculated for each participant and then averaged across participants. Inset shows the color scale for the data matrices. In each matrix, tasks are ordered (top to bottom and left to right) as follows: 1) theory of mind, 2) moral dilemmas, 3) autobiographical memory, 4) spatial imagery, 5) self/other, and 6) rest. To the right of each data matrix are shown correlations with four model similarity matrices (top of each column). From left to right, the models represent: high similarity for "mental state" tasks (Model 1), high similarity for "memory-based construction/simulation" tasks (Model 2), high dissimilarity of self–other to all other tasks (Model 3), high dissimilarity of rest minus task to other contrasts (Model 4). In the model matrices, white indicates empty cells not used in the comparisons, gray indicates ones (similar), and black indicates zeros (dissimilar). Bar graphs indicate the Kendall's tau-a correlation between each participant's empirical and model similarity matrices tested against zero (corrected for multiple comparisons at FDR < 0.05; *** indicates $P < 0.001$, ** indicates $P < 0.01$, and * indicates $P < 0.05$). (2) Equivalent results averaged across ROIs within each subnetwork. (B) Dissimilarity matrix calculated using 1 − Pearson's correlation between ROIs based on their correlation profiles across 15 task pairs. (C) MDS to visualize the dissimilarity between regions. L- and R- indicate left and right.

differences. The vMPFC showed an activity profile that was shifted toward that of aMPFC, while the pIPL responded to most contrasts (Fig. 4). Analysis of multivoxel patterns showed a largely similar picture. For MTL regions except vMPFC, voxelwise activity patterns were especially similar for the memory and imagery contrasts (Fig. 5A). Across all task pairs, profiles of between-task distances were largely similar for the posterior medial regions (Fig. 5B, C). Again, though, the distance profile of pIPL was rather different, with some similarity to other regions of both MTL and dMPFC subsystems, and, again, vMPFC was shifted toward aMPFC (Fig. 5B, C).

Our results give less clear-cut support to the concept of a midline core consisting of aMPFC and PCC. In terms of both univariate and multivariate activity, aMPFC was more similar to the adjacent dMPFC and vMPFC regions than to PCC. In terms of univariate activity, its strongest response was to the self–other contrast (Fig. 4A). Intriguingly, aMPFC was also the region showing most widespread deactivations compared to rest, suggesting especially strong involvement in operations that take place with no active task. In contrast, both univariate and multivariate analyses placed PCC between dMPFC and MTL subsystems, with results closely similar to those of pIPL (Figs 4C and 5C). If anything, these results suggest pIPL and PCC as a DMN functional "core", while MPFC regions show some dorsal–ventral gradient but also resemblances to one another, and relatively distinct profiles compared to the other ROIs, including PCC. Though assigning pIPL to the DMN core is not in line with the original scheme of Andrews-Hanna et al. (2010), it does match later suggestions from the same group (Andrews-Hanna et al. 2014b). In this revised scheme, based on resting state connectivity data from Yeo et al. (2011), Andrews-Hanna et al. (2014b) also assign a large part of pIPL to the DMN core.

Some important general caveats should be considered. Undoubtedly, our *a priori* ROIs would not match the exact functional regions of individual participants, meaning that results for adjacent regions will to some extent blur together. One region where this consideration could be especially significant is the inferior parietal lobule, represented here by pIPL and TPJ ROIs (Fig. 2). Although our univariate data agreed with the proposals of Andrews-Hanna et al. (2010) in separating pIPL and TPJ, some blurring between these functionally separate regions might have contributed to TPJ's response to autobiographical memory and spatial imagery contrasts, and the pIPL's multivoxel pattern similarity to both dMPFC and MTL subsystems. The same might also apply to our finding of broad similarities between the three MPFC regions, though, despite these concerns, our results did confirm some dorsal–ventral gradient, with the dMPFC being more involved in tasks requiring "introspection of mental states" and vMPFC more involved in tasks requiring "memory-based construction/simulation".

Other aspects of our results cannot be explained by spatial blurring. In particular, a conspicuous result was a significant response to nonsocial contrasts throughout most regions of the dMPFC subsystem, including those far from the MTL or core hubs. Along with the broad similarity of whole-brain maps for each contrast (Fig. 3), apart from self > other, such results confirm partial, but not complete separation of response patterns for different DMN subsystems. Furthermore, using smaller and more focal spherical ROIs generated around peak coordinates from Andrews-Hanna et al. (2010) gave similar overall results (Supplementary Figs 1 and 3).

Another possible concern is the cognitive separation of the six tasks. Although we picked tasks that were hypothesized to preferentially engage processes related to specific subsystems, the possibility remains that tasks also engaged functions beyond those of the targeted subsystem. While all tasks were predicted to engage the core, the theory of mind and moral dilemmas tasks aimed to minimize activation of the MTL subsystem, while the autobiographical memory and spatial imagery tasks aimed to avoid the dMPFC subsystem. Regarding theory of mind and moral reasoning, the data suggest that we were largely successful, with little or no activity in much of the MTL subsystem, including Rsp, PHC, and HF+. For autobiographical memory, it is plausible to assign activity in the dMPFC subsystem to the social content of many memories. This interpretation is less appealing for the spatial imagery contrast, since neither the imagery nor the digit control task had an evident social component, but association of the dMPFC subsystem with wider aspects of semantic cognition (Andrews-Hanna et al. 2014b) offers a further potential aspect of task impurity. In future work, such issues could be more fully addressed with a larger set of task contrasts.

While subsystems and component ROIs showed preferences for different tasks, there is evidence for further structure within them. Our task-wise multivoxel pattern similarity analysis (Fig. 5), showing that tasks of the same cognitive domain had higher pattern similarity, indicates fine-scale patterns for different types of tasks within our ROIs. In addition to subnetworks, previous studies have also suggested fractionation within a single region (Leech et al. 2011; Nelson et al. 2012; Peer et al. 2015; Chrastil 2018; Silson et al. 2019); for example, a posterior–anterior axis of activation for orienting to space, person, and time in the precuneus and IPL (Peer et al. 2015). Of particular relevance here are the results of Braga and Buckner (2017), who scanned four individuals 24 times using fMRI. The authors found that two distinct networks that resembled the dMPFC and MTL subsystems in Andrews-Hanna et al. (2010) could be identified in each individual. However, spatially juxtaposed regions of the two networks were found in each of the three MPFC regions: dMPFC, aMPFC, and vMPFC, which may be blurred together by spatial averaging in a group analysis. Together, these results demonstrate a coarse, partial division into subnetworks as proposed by Andrews-Hanna et al. (2010), as well as fine-scale separations by task content within each region.

As noted earlier, several authors have proposed that the DMN represents broad features of a cognitive episode, situation or context (Hassabis and Maguire 2007; Ranganath and Ritchey 2012; Manning et al. 2014). Our results suggest both partial functional separation but also integration within this context representation. Matching many other findings (Andrews-Hanna et al. 2014a; Axelrod et al. 2017), our results link regions of the dMPFC subsystem to social cognition, and regions of the MTL subsystem to spatial or scene representation. To represent a cognitive episode, it is plausible that social and spatial representations are often integrated (Andrews-Hanna et al. 2014b; Peer et al. 2015), for example, to indicate who is where in the represented episode. Such integration may be achieved through communication between dMPFC and MTL subsystems, perhaps especially mediated by the pIPL and PCC. The self is also likely to be a core part of any episode representation, perhaps especially dependent on MPFC. In this way, the DMN acts partly as an integrated whole, but binding together aspects of the episode representation that are predominantly contributed by separate subregions.

Two other regions are worthy of further consideration. The first is the inferior frontal gyrus (IFG) that was not part of

our a priori ROIs. Our whole-brain results (Fig. 3A) showed that although IFG activity was weak in second-level analyses for most tasks (with the exception of self > other), a substantial minority of individual participants showed reliable recruitment for most tasks (Fig. 3B). In studies of semantic processing, activity in regions of the dMPFC subsystem is often accompanied by IFG activity, leading to its inclusion in a proposed "semantic control network" (Binder et al. 2009; Noonan et al. 2013). Based on the resting state data of Yeo et al. (2011), Andrews-Hanna et al. (2014b) also include IFG in the dMPFC subsystem. Given these findings, future studies should consider further the relation between social cognition and the semantic control network, including the IFG. One possibility is that the IFG acts as a gateway to the DMN, via the semantic control network, when semantic retrieval is constrained by external stimuli (Chiou et al. 2019).

The second region requiring further consideration is the hippocampus. The hippocampal peak (HF+) defined in Andrews-Hanna et al. (2010) is not located in the hippocampus proper, but lies between the PHC and perirhinal cortex (PRC) (Moore et al. 2014; Ritchey et al. 2015; https://neurovault.org/collections/3731/). The PHC has been linked to the "posterior medial system", a network closely related to the DMN, while the PRC has been linked to the "anterior temporal system", along with the TempP and orbitofrontal cortex (Ranganath and Ritchey 2012). The role of the current HF+ ROI is therefore unclear as it may span functionally heterogeneous regions. Another question is whether the hippocampus is part of the DMN at all. Our results show a mixed picture, as only some contrasts activated parts of the hippocampus. Although the hippocampus has been associated with episodic memory and spatial navigation (Maguire et al. 1998; Addis et al. 2007; Rugg et al. 2012; Brown et al. 2016), it has been proposed to play a different role from other regions in the MTL subsystem. In particular, the hippocampus may integrate information across the anterior temporal and posterior medial systems (Ranganath and Ritchey 2012).

Our findings provide a mixed answer to the question of functional specialization within the DMN. On the one hand, there is evidence of a largely integrated whole, with similar whole-brain activity maps for multiple contrasts, and some response to every contrast in each of the proposed subsystems, supporting classical accounts (e.g., Buckner and Carroll 2007; Spreng et al. 2009). On the other hand, there is partial functional separation for different kinds of DMN-related processing. At a coarse scale, separation is in broad accord with the proposals of separate dMPFC and MTL subsystems (Andrews-Hanna et al. 2010; Andrews-Hanna 2012; Andrews-Hanna et al. 2014a), though with remaining uncertainties over the concept of a midline core. At a finer scale, there is evidence that, within subsystems and even within individual ROIs, different types of cognitive operation produce different local patterns of activity. Combining separation and integration of social, spatial, self-related, and other aspects of a cognitive situation or episode, the DMN may provide the broad context for current mental activity.

Supplementary Material

Supplementary material can be found at *Cerebral Cortex* online.

Funding

Medical Research Council (UK) program (SUAG/002/RG91365). T.W. was supported by the Medical Research Council studentship and the Percy Lander studentship from Downing College.

Conflict of Interest

None declared.

References

Addis DR, Wong AT, Schacter DL. 2007. Remembering the past and imagining the future: common and distinct neural substrates during event construction and elaboration. *Neuropsychologia*. 45:1363–1377.

Anderson NH. 1968. Likableness ratings of 555 personality-trait words. *Journal of personality and social psychology*. 9:272.

Andrews-Hanna JR. 2012. The brain's default network and its adaptive role in internal mentation. *Neuroscientist*. 18:251–270.

Andrews-Hanna JR, Reidler JS, Sepulcre J, Poulin R, Buckner RL. 2010. Functional-anatomic fractionation of the brain's default network. *Neuron*. 65:550–562.

Andrews-Hanna JR, Saxe R, Yarkoni T. 2014a. Contributions of episodic retrieval and mentalizing to autobiographical thought: evidence from functional neuroimaging, resting-state connectivity, and fMRI meta-analyses. *Neuroimage*. 91:324–335.

Andrews-Hanna JR, Smallwood J, Spreng RN. 2014b. The default network and self-generated thought: component processes, dynamic control, and clinical relevance. *Ann N Y Acad Sci*. 1316:29–52.

Axelrod V, Rees G, Bar M. 2017. The default network and the combination of cognitive processes that mediate self-generated thought. *Nat Hum Behav*. 1:896–910.

Baldassano C, Chen J, Zadbood A, Pillow JW, Hasson U, Norman KA. 2017. Discovering event structure in continuous narrative perception and memory. *Neuron*. 95:709–721.e5.

Benjamini Y, Yekutieli D. 2001. The control of the false discovery rate in multiple testing under dependency. *Ann Stat*. 29:1165–1188.

Binder JR, Desai RH, Graves WW, Conant LL. 2009. Where is the semantic system? A critical review and meta-analysis of 120 functional neuroimaging studies. *Cereb Cortex*. 19:2767–2796.

Braga RM, Buckner RL. 2017. Parallel interdigitated distributed networks within the individual estimated by intrinsic functional connectivity. *Neuron*. 95:457–471.e5.

Brainard DH. 1997. The psychophysics toolbox. *Spatial vision*. 10:433–436.

Brett M, Anton JL, Valabregue R, Poline JB. 2002. Region of interest analysis using an SPM toolbox. *In 8th international conference on functional mapping of the human brain*. 16:497.

Brown TI, Carr VA, LaRocque KF, Favila SE, Gordon AM, Bowles B, Bailenson JN, Wagner AD. 2016. Prospective representation of navigational goals in the human hippocampus. *Science*. 352:1323–1326.

Buckner RL, Andrews-Hanna JR, Schacter DL. 2008. The brain's default network: anatomy, function, and relevance to disease. *Ann N Y Acad Sci*. 1124:1–38.

Buckner RL, Carroll DC. 2007. Self-projection and the brain. *Trends Cogn Sci*. 11:49–57.

Chiou R, Humphreys GF, Lambon Ralph MA. 2020. Bipartite Functional Fractionation within the Default Network Supports Disparate Forms of Internally Oriented Cognition. *Cereb Cortex*. bhaa130. doi: 10.1093/cercor/bhaa130.

Chrastil ER. 2018. Heterogeneity in human retrosplenial cortex: a review of function and connectivity. *Behav Neurosci*. 132:317–338.

Christoff K, Gordon AM, Smallwood J, Smith R, Schooler JW. 2009. Experience sampling during fMRI reveals default network and executive system contributions to mind wandering. *Proc Natl Acad Sci U S A*. 106:8719–8724.

Christoff K, Ream JM, Gabrieli JDE. 2004. Neural basis of spontaneous thought processes. *Cortex*. 40:623–630.

Crittenden BM, Mitchell DJ, Duncan J. 2015. Recruitment of the default mode network during a demanding act of executive control. *Elife*. 2015:1–12.

Cusack R, Vicente-Grabovetsky A, Mitchell DJ, Wild CJ, Auer T, Linke AC, Peelle JE. 2015. Automatic analysis (aa): efficient neuroimaging workflows and parallel processing using Matlab and XML. *Frontiers in neuroinformatics*. 8:90.

Dodell-Feder D, Koster-Hale J, Bedny M, Saxe R. 2011. fMRI item analysis in a theory of mind task. *Neuroimage*. 55:705–712.

Fedorenko E, Duncan J, Kanwisher N. 2013. Broad domain generality in focal regions of frontal and parietal cortex. *Proceedings of the National Academy of Sciences*. 110:16616–16621.

Frith CD, Frith U. 2006. The neural basis of mentalizing. *Neuron*. 50:531–534.

Greene J, Haidt J. 2002. How (and where) does moral judgment work? *Trends Cogn Sci*. 6:517–523.

Greene JD, Sommerville RB, Nystrom LE, Darley JM, Cohen JD. 2001. An fMRI investigation of emotional engagement in moral judgment. *Science*. 293:2105–2108.

Hassabis D, Maguire EA. 2007. Deconstructing episodic memory with construction. *Trends Cogn Sci*. 11:299–306.

Heller R, Golland Y, Malach R, Benjamini Y. 2007. Conjunction group analysis: an alternative to mixed/random effect analysis. *Neuroimage*. 37:1178–1185.

Humphreys GF, Lambon Ralph MA. 2017. Mapping domain-selective and counterpointed domain-general higher cognitive functions in the lateral parietal cortex: evidence from fMRI comparisons of difficulty-varying semantic versus visuo-spatial tasks, and functional connectivity analyses. *Cereb Cortex*. 27:4199–4212.

Kelley WM, Macrae CN, Wyland CL, Caglar S, Inati S, Heatherton TF. 2002. Finding the self? An event-related fMRI study. *J Cogn Neurosci*. 14:785–794.

Lambon Ralph MA, Jefferies E, Patterson K, Rogers TT. 2017. The neural and computational bases of semantic cognition. *Nat Rev Neurosci*. 18:42–55.

Leech R, Kamourieh S, Beckmann CF, Sharp DJ. 2011. Fractionating the default mode network: distinct contributions of the ventral and dorsal posterior cingulate cortex to cognitive control. *J Neurosci*. 31:3217–3224.

Maguire EA, Burgess N, Donnett JG, Frackowiak RS, Frith CD, O'Keefe J. 1998. Knowing where and getting there: a human navigation network. *Science*. 280:921–924.

Manning JR, Kahana MJ, Norman KA. 2014. The role of context in episodic memory. In: Gazzaniga ME, editor. *The cognitive neurosciences*. 5th ed. Cambridge, MA: MIT Press.

Mars RB, Neubert F-X, Noonan MP, Sallet J, Toni I, Rushworth MFS. 2012. On the relationship between the "default mode network" and the "social brain". *Front Hum Neurosci*. 6:189.

McDermott KB, Szpunar KK, Christ SE. 2009. Laboratory-based and autobiographical retrieval tasks differ substantially in their neural substrates. *Neuropsychologia*. 47:2290–2298.

Molenberghs P, Johnson H, Henry JD, Mattingley JB. 2016. Understanding the minds of others: a neuroimaging meta-analysis. *Neurosci Biobehav Rev*. 65:276–291.

Moore M, Hu Y, Woo S, O'Hearn D, Iordan AD, Dolcos S, Dolcos F. 2014. A comprehensive protocol for manual segmentation of the medial temporal lobe structures. *JoVE (Journal of Visualized Experiments)*. e50991.

Nelson SM, McDermott KB, Petersen SE. 2012. In favor of a 'fractionation' view of ventral parietal cortex: comment on Cabeza et al. *Trends Cogn Sci*. 16:399–400.

Nili H, Wingfield C, Walther A, Su L, Marslen-Wilson W, Kriegeskorte N. 2014. A toolbox for representational similarity analysis. *PLoS computational biology*. 10.

Noonan KA, Jefferies E, Visser M, Lambon Ralph MA. 2013. Going beyond inferior prefrontal involvement in semantic control: evidence for the additional contribution of dorsal angular gyrus and posterior middle temporal cortex. *J Cogn Neurosci*. 25:1824–1850.

Peer M, Salomon R, Goldberg I, Blanke O, Arzy S. 2015. Brain system for mental orientation in space, time, and person. *Proc Natl Acad Sci U S A*. 112:11072–11077.

Raichle ME, MacLeod AM, Snyder AZ, Powers WJ, Gusnard DA, Shulman GL. 2001. A default mode of brain function. *Proc Natl Acad Sci*. 98:676–682.

Ranganath C, Ritchey M. 2012. Two cortical systems for memory-guided behaviour. *Nat Rev Neurosci*. 13:713–726.

Ritchey M, Montchal ME, Yonelinas AP, Ranganath C. 2015. Delay-dependent contributions of medial temporal lobe regions to episodic memory retrieval. *Elife*. 4:e05025.

Rorden C, Karnath HO, Bonilha L. 2007. Improving lesion-symptom mapping. *J Cogn Neurosci*. 19:1081–1088.

Rugg MD, Vilberg KL. 2013. Brain networks underlying episodic memory retrieval. *Curr Opin Neurobiol*. 23:255–260.

Rugg MD, Vilberg KL, Mattson JT, Yu SS, Johnson JD, Suzuki M. 2012. Item memory, context memory and the hippocampus: fMRI evidence. *Neuropsychologia*. 50:3070–3079.

Shulman GL, Fiez JA, Corbetta M, Buckner RL, Miezin FM, Raichle ME, Petersen SE. 1997. Common blood flow changes across visual tasks: II. Decreases in cerebral cortex. *J Cogn Neurosci*. 9:648–663.

Silson EH, Steel A, Kidder A, Gilmore AW, Baker CI. 2019. Distinct subdivisions of human medial parietal cortex support recollection of people and places. *Elife*. 8:e47391.

Smith V, Mitchell DJ, Duncan J. 2018. Role of the default mode network in cognitive transitions. *Cereb Cortex*. 28:3685–3696.

Speer ME, Delgado MR. 2019. The social value of positive autobiographical memory retrieval. *J Exp Psychol Gen*. 149: 790–799.

Spreng RN, Grady CL. 2010. Patterns of brain activity supporting autobiographical memory, prospection, and theory of mind, and their relationship to the default mode network. *J Cogn Neurosci*. 22:1112–1123.

Spreng RN, Mar RA, Kim ASN. 2009. The common neural basis of autobiographical memory, prospection, navigation, theory of mind, and the default mode: a quantitative meta-analysis. *J Cogn Neurosci*. 21:489–510.

Vass LK, Epstein RA. 2017. Common neural representations for visually guided reorientation and spatial imagery. *Cereb cortex*. 27:1457–1471.

Yeo BT, Krienen FM, Sepulcre J, Sabuncu MR, Lashkari D, Hollinshead M, Roffman JL, Smoller JW, Zöllei L, Polimeni JR *et al*. 2011. The organization of the human cerebral cortex estimated by intrinsic functional connectivity. *J Neurophysiol*. 106:1125–1165.